

# Circulation

JOURNAL OF THE AMERICAN HEART ASSOCIATION



## Assessment of the Tissue Distribution of Transplanted Human Endothelial Progenitor Cells by Radioactive Labeling

Alexandra Aicher, Winfried Brenner, Maaz Zuhayra, Cornel Badorff, Schirin Massoudi, Birgit Assmus, Thomas Eckey, Eberhard Henze, Andreas M. Zeiher and Stefanie Dimmeler

*Circulation* published online Apr 14, 2003;

DOI: 10.1161/01.CIR.0000062649.63838.C9

*Circulation* is published by the American Heart Association, 7272 Greenville Avenue, Dallas, TX 75214

Copyright © 2003 American Heart Association. All rights reserved. Print ISSN: 0009-7322. Online ISSN: 1524-4539

The online version of this article, along with updated information and services, is located on the World Wide Web at:

<http://circ.ahajournals.org>

Subscriptions: Information about subscribing to *Circulation* is online at  
<http://circ.ahajournals.org/subscriptions/>

Permissions: Permissions & Rights Desk, Lippincott Williams & Wilkins, a division of Wolters Kluwer Health, 351 West Camden Street, Baltimore, MD 21202-2436. Phone: 410-528-4050. Fax: 410-528-8550. E-mail:  
[journalpermissions@lww.com](mailto:journalpermissions@lww.com)

Reprints: Information about reprints can be found online at  
<http://www.lww.com/reprints>

## Assessment of the Tissue Distribution of Transplanted Human Endothelial Progenitor Cells by Radioactive Labeling

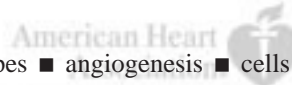
Alexandra Aicher, MD\*; Winfried Brenner, MD\*; Maaz Zuhayra, PhD; Cornel Badorff, MD; Schirin Massoudi, MD; Birgit Assmus, MD; Thomas Eckey; Eberhard Henze, MD; Andreas M. Zeiher, MD; Stefanie Dimmeler, PhD

**Background**—Transplantation of endothelial progenitor cells (EPCs) improves vascularization and left ventricular function after experimental myocardial ischemia. However, tissue distribution of transplanted EPCs has not yet been monitored in living animals. Therefore, we tested whether radioactive labeling allows us to detect injected EPCs.

**Methods and Results**—Human EPCs were isolated from peripheral blood, characterized by expression of endothelial marker proteins, and radioactively labeled with [<sup>111</sup>In]indium oxine. EPCs (10<sup>6</sup>) were injected in athymic nude rats 24 hours after myocardial infarction (n=8) or sham operation (n=8). Scintigraphic images were acquired after 1, 24, 48, and 96 hours after EPC injection. Animals were then killed, and specific radioactivity was measured in different tissues. At 24 to 96 hours after intravenous injection of EPCs, ≈70% of the radioactivity was localized in the spleen and liver, with only ≈1% of the radioactivity identified in the heart of sham-operated animals. After myocardial infarction, the heart-to-muscle radioactivity ratio increased significantly, from 1.02±0.19 in sham-operated animals to 2.03±0.37 after intravenous administration of EPCs. Injection of EPCs into the left ventricular cavity increased this ratio profoundly, from 2.69±1.54 in sham-operated animals to 4.70±1.55 (*P*<0.05) in rats with myocardial infarction. Immunostaining of cryosections from infarcted hearts confirmed that EPCs homed predominantly to the infarct border zone.

**Conclusions**—Although only a small proportion of radiolabeled EPCs are detected in nonischemic myocardium, myocardial infarction increases homing of transplanted EPCs in vivo profoundly. Radiolabeling might eventually provide an useful tool for monitoring the fate of transplanted progenitor cells and for clinical cell therapy. (*Circulation*. 2003;107:2134-2139.)

**Key Words:** myocardial infarction ■ imaging ■ radioisotopes ■ angiogenesis ■ cells



Endothelial progenitor cells (EPCs) can contribute to neovascularization of ischemic heart tissue. Infusion of ex vivo-cultivated EPCs was shown to improve vascularization and left ventricular function after myocardial ischemia.<sup>1,2</sup> The integration of EPCs into the neovasculature of ischemic regions has been documented by use of immunohistochemical staining of tissue sections.<sup>1-3</sup> Biodistribution of transplanted EPCs in vivo was followed up either by uptake of red fluorescence-labeled acetylated LDL (DiLDL) or by genetic modifications introducing genes for fluorochromes or metabolic enzymes.<sup>2,4,5</sup> However, detection of fluorescence or enzyme-produced colorimetric reactions is a laborious process limited by the need to take biopsies or kill the animal, which precludes its use in humans. In addition, immunohistochemical analysis of tissue sections is severely limited to assess the temporal course of homing and tissue distribution

of transplanted cells within the whole body. Therefore, the development of noninvasive imaging approaches for monitoring the fate and tissue distribution of transplanted progenitor cells is required.

One approach to track the distribution pattern of in vivo-injected cells is the monitoring of cells after radiolabeling. [<sup>111</sup>In]indium oxine (<sup>111</sup>In-oxine) has been widely accepted for safe radiolabeling of leukocytes to localize areas of inflammation.<sup>6-8</sup> Moreover, <sup>111</sup>In-oxine has been used to determine the biodistribution of transplanted hepatocytes<sup>9</sup> or dendritic cells.<sup>10,11</sup> Therefore, we investigated whether radioactive labeling with <sup>111</sup>In-oxine might provide a clinically applicable tool to monitor the fate of transplanted EPCs in living rats after myocardial infarction. Moreover, we examined whether the route of administration, ie, intravenous versus left ventricular intracavitary application, affects myocardial incorporation of EPCs.

Received November 21, 2002; revision received January 21, 2003; accepted January 21, 2003.

From the Department of Molecular Cardiology (A.A., C.B., B.A., A.M.Z., S.D.), Department of Internal Medicine IV, University of Frankfurt, and the Department of Nuclear Medicine (W.B., M.Z., S.M., T.E., E.H.), University of Kiel, Germany.

\*The first 2 authors contributed equally to this work.

Correspondence to Stefanie Dimmeler, PhD, Molecular Cardiology, Department of Internal Medicine IV, University of Frankfurt, Theodor Stern-Kai 7, 60590 Frankfurt, Germany. E-mail dimmeler@em.uni-frankfurt.de

© 2003 American Heart Association, Inc.

*Circulation* is available at <http://www.circulationaha.org>

DOI: 10.1161/01.CIR.0000062649.63838.C9

## Methods

### Cell Culture

Ex vivo expansion of EPCs was performed according to Vasa et al<sup>12</sup> in a modification that also used 50 ng/mL vascular endothelial growth factor (Peprotech), 20 ng/mL basic fibroblast growth factor (R&D), and 0.1  $\mu$ mol/L atorvastatin (Pfizer). Vascular endothelial growth factor, basic fibroblast growth factor, and atorvastatin were used to increase EPC numbers as described previously.<sup>12,13</sup>

### Fluorescence and Radioactive Labeling

Adherent EPCs were detached with 1 mmol/L EDTA, pH 7.4, for 15 minutes at 37°C. After a washing with PBS, the pelleted cells were adjusted to  $6 \times 10^6$ /mL and labeled with 4  $\mu$ g/mL DiLDL for 20 minutes at 37°C. EPCs were washed with PBS and resuspended in growth factor and serum-free endothelial basal medium (EBM). Then  $10^6$  EPCs/mL were labeled with 15 MBq of <sup>111</sup>In-oxine (physical half-life, 2.8 days;  $\gamma$ -energy, 171 keV, 245 keV; 37 MBq/mL; Mallinckrodt) for 60 minutes at 37°C. To remove excess unbound radioactivity, cells were washed twice. Labeling efficiency was measured with a dose calibrator (Atomlab 100, Biodex Medical). Before injection, EPCs were resuspended in 0.5 mL serum-free EBM in 1.0-mL syringes with 27-gauge needles.

### Assessment of Cell Viability

LDH release (cytotoxicity detection kit [LDH], Roche) in the supernatants of <sup>111</sup>In-oxine-labeled cells was measured to evaluate cell death and compared with untreated controls.

DiLDL uptake as a functional assay for EPC viability was performed. <sup>111</sup>In-oxine-labeled EPCs underwent DiLDL labeling and were fixed in 2% formaldehyde. The number of DiLDL<sup>+</sup> cells was determined with a fluorescence microscope (Axiovert 100 M, Zeiss) and evaluated by counting 3 randomly selected high-power fields.

### Migration Assay

Migration assays were performed with  $2 \times 10^4$  radiolabeled or unlabeled EPCs in 0.2 mL EBM that were seeded into the top chamber of a modified Boyden chamber, as described previously.<sup>12</sup>

### Animal Experiments

Because of the transplantation of human EPCs into a xenogeneic rat model, immunodeficient athymic rnu:rnu rats (5- to 7-week-old females; Charles River, Sulzfeld, Germany) were required. Animals were anesthetized with intramuscular ketamine (100 mg/kg; Curamed) and midazolam (2 mg/kg; Hoffmann-La-Roche). To prevent arrhythmias after cardiac surgery, intramuscular amiodarone (5 mg/kg; Sanofi-Syhelabo) was given prophylactically. An endotracheal tube (17-gauge) was inserted for volume-controlled ventilation of the animals. Open-chest cardiac surgery was performed after left thoracotomy to occlude the left coronary artery by passing a 5-0 suture just under the tip of the left auricle (n=8). Sham-treated animals underwent left thoracotomy and incision of the pericardium (n=8). To reduce postoperative pain, piritramide (2 mg/kg; Janssen-Cilag) was administered. After the chest wound was closed, rnu:rnu rats were allowed to recover for 24 hours before injection of EPCs. DiLDL and <sup>111</sup>In-oxine-labeled EPCs were given either by intravenous application into the lateral tail vein (n=8) or with a x-ray-assisted transdiaphragmatic approach for administration into the left ventricular cavity (n=8). Before the latter procedure, contrast medium (Isovist, Schering) was injected transdiaphragmatically into the heart to check left ventricular position under radiographic control. Furthermore, 3 additional animals received free <sup>111</sup>In-oxine as radioactivity-positive controls.

Scintigrams of the animals were acquired immediately after tracer injection with a double-headed gamma camera (ECAM, Siemens) equipped with a pinhole collimator with an inset for medium energy. The energy windows were centered at 171 keV $\pm$ 10% and 245 keV $\pm$ 10%.

All animal experiments were performed with approved consent by the Animal Research Committee at the University of Kiel in accordance with federal law (V 252-72241.122-17).

### Tissue Preparation and Immunostaining

Hearts of the euthanized animals were perfused with heparinized saline through the cannulated abdominal aorta. Transverse slices of the base, midregion, and apex of the hearts as well as tissue samples from other organs, such as skeletal muscles, lungs, kidneys, liver, and spleen, were obtained. All specimens were weighed, and the count rate was measured in a lead-shielded and calibrated well counter (LB 5310, Berthold) to calculate the specific activity per gram tissue sample after correction for radioactive decay. Furthermore, organ samples were mounted in OCT compound (TissueTek, Sakura) and snap-frozen in liquid nitrogen. Sections (5  $\mu$ m) were then cut and examined for red fluorescent DiLDL-labeled EPCs in the native specimens. To confirm the human origin of the EPCs found in the frozen tissue sections, we used FITC- or phycoerythrin-labeled anti-HLA class I (1:50; Caltag) that specifically recognizes human but not rat major histocompatibility class I molecules. In addition, double-staining with rhodamine-labeled *Ulex europaeus* lectin (1:150; Vector Laboratories) was performed to confirm the endothelial character of the detected cells. Destruction of cardiac myocytes after myocardial infarction was visualized by staining of myocytes with FITC-conjugated (Pierce)  $\alpha$ -sarcomeric actinin (1:250; Sigma). For immunostaining, sections were incubated with the directly fluorochrome-conjugated antibodies for 1 hour at room temperature. PBS was used for washing between the subsequent incubation steps. Fluorescence was visualized with an Axiovert 100 M microscope (Zeiss) equipped with a digital camera (AxioCam; Zeiss) and imaging software (Axiovision; Zeiss).

### Statistical Analysis

Data are expressed as mean $\pm$ SD. Unpaired, 2-tailed *t* test was used for the comparison of continuous variables. A value of *P*<0.05 was considered statistically significant.

## Results

### In Vitro Labeling of EPCs With <sup>111</sup>In-oxine

Human EPCs were cultivated, and the endothelial phenotype was confirmed by demonstration of endothelial marker proteins such as VE-cadherin, KDR, von Willebrand factor, and endothelial nitric oxide synthase as previously described.<sup>12,13</sup>

To test the efficiency of the labeling, EPCs were incubated with 15 MBq <sup>111</sup>In-oxine in serum-free EBM between 10 and 60 minutes. A time-dependent incorporation of <sup>111</sup>In-oxine was observed with a maximum efficiency after 60 minutes (Figure 1A), resulting in an overall labeling efficiency of 67 $\pm$ 13%. Next, we investigated whether the labeling affects cell viability or function. Therefore, LDH release was measured as a marker for cell death in the cell culture supernatant. However, up to 96 hours after <sup>111</sup>In-oxine labeling, LDH activity in the replated radiolabeled EPCs was not significantly different from controls, with 96.3 $\pm$ 5.7% of unlabeled cells at 96 hours after labeling (n=3). Moreover, the functional activity of EPCs was assessed by DiLDL uptake. The number of cells that actively took up DiLDL was 93.4 $\pm$ 3.9% (n=3) of the number of DiLDL<sup>+</sup> cells in unlabeled EPCs after 48 hours and 90.2 $\pm$ 4.7% after 96 hours (n=3). Similarly, the functional capacity of EPCs to migrate in response to vascular endothelial growth factor in a modified Boyden chamber assay was not affected by radiolabeling when radiolabeled EPCs were compared with their unlabeled controls (Figure 1B). To determine the leakage of <sup>111</sup>In into the supernatant,

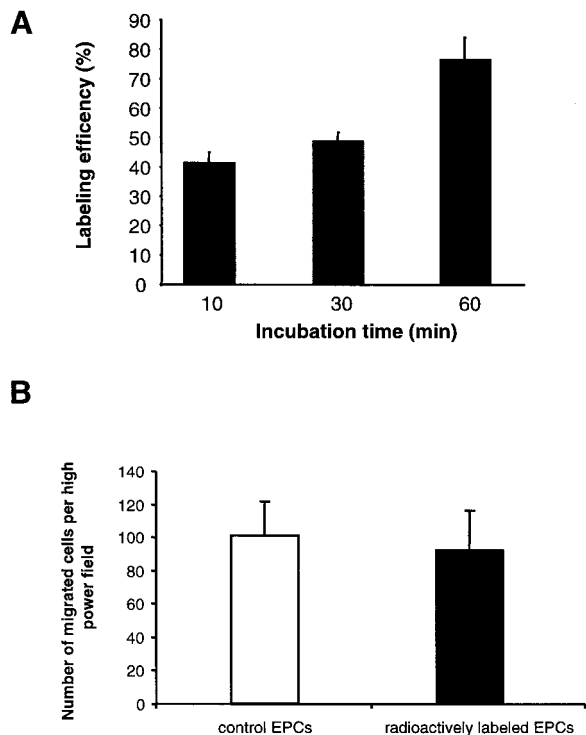


**Figure 1.** In vitro assays using  $^{111}\text{In}$ -oxine-labeled EPCs. A, Time course of labeling efficiency of EPCs with 15 MBq  $^{111}\text{In}$ -oxine. B, In addition, radiolabeling did not affect functional capacity of EPCs to migrate, as assessed by a modified Boyden chamber assay. Data are given as mean  $\pm$  SD ( $n=3$ ).

we checked the activity of  $^{111}\text{In}$  in the supernatants as well as in the adherently growing EPCs. We found that  $39.3 \pm 2.1\%$  of the  $^{111}\text{In}$  incorporated into EPCs was retained after 48 hours and  $22.0 \pm 7.5\%$  after 96 hours.

### Distribution of EPCs in Rats

In the first set of experiments, radioactively labeled human EPCs were infused intravenously in sham-operated ( $n=4$ ) or infarcted ( $n=4$ ) athymic immunodeficient nude rats. Scintigraphic images of the animals were acquired with a gamma

camera with pinhole collimators (Figure 2). Images were obtained after injection and then 24, 48, and 96 hours later.

Immediately after injection of the EPCs, a high tracer accumulation was found in the liver, kidneys, and spleen, which increased to  $71.8 \pm 13.7\%$  of the injected activity at 60 minutes. No radioactivity was visible in bones, suggesting that EPCs do not accumulate in the bone marrow to a significant extent within the first 24 hours. The tracer distribution did not show major changes up to 96 hours after injection, at which time  $71.0 \pm 7.1\%$  of the whole-body activity was detectable in liver, kidneys, and spleen. Furthermore, there was still no bone marrow uptake. Using a pinhole collimator, the increase in ischemia-induced heart uptake compared with sham-operated controls is readily visible (Figure 2). After 96 hours, animals were killed, and the specific radioactivity was measured in different tissues. Consistent with the in vivo images, the majority of the radioactivity was detected in spleen and liver (Figure 3A) after intravenous injection. In sham-operated animals, only  $\approx 1\%$  of the injected radioactivity was detected in the heart. The specific heart radioactivity was  $9543 \pm 1142$  cpm/g tissue. The ratio of specific radioactivity of the heart compared with peripheral skeletal muscle tissue was  $1.02 \pm 0.19$  in sham-operated animals. After the induction of myocardial infarction, this ratio increased significantly, to  $2.03 \pm 0.37$  ( $P < 0.05$ ) (Figure 3B) according to a specific heart activity of  $28\,376 \pm 1851$  cpm/g ( $P < 0.05$ ).

To investigate whether a local administration of EPCs increased the homing of EPCs to the heart, EPCs were injected into the left ventricular cavity. Overall, a similar distribution of radioactive EPCs was found (Figure 3A). However, both the heart specific radioactivity and the heart-to-muscle specific radioactivity ratio were increased significantly, to  $24\,192 \pm 7097$  cpm/g tissue and  $2.69 \pm 1.54$ , respectively, in sham-operated animals when EPCs were injected into the left ventricular cavity compared with intravenous infusion (Figure 3B). Moreover, the heart-to-muscle specific radioactivity ratio increased further, to  $4.70 \pm 1.55$ , with a specific heart radioactivity of  $57\,273 \pm 22\,418$  cpm/g tissue ( $P < 0.05$  versus sham-operated) when EPCs were infused

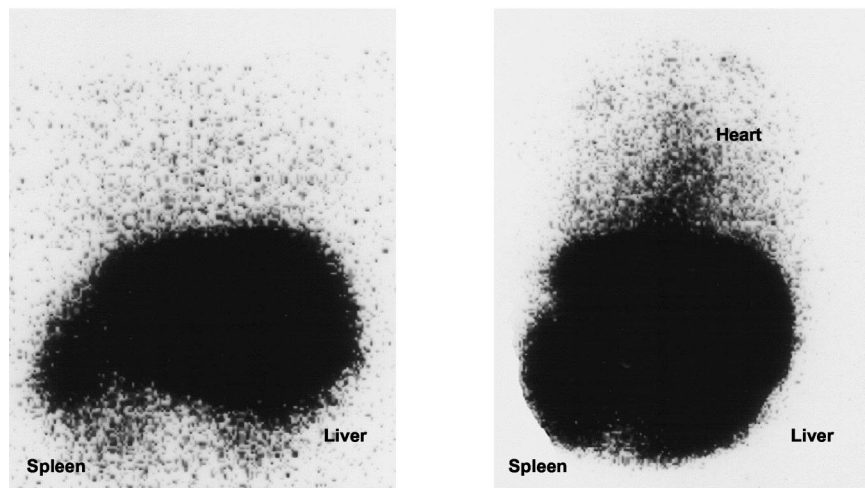


**Figure 2.** Scintigraphic pinhole images of the thorax and abdomen of nude rats with or without (sham-operated) myocardial infarction from posterior view 24 hours after injection of  $^{111}\text{In}$ -oxine-labeled EPCs. Representative scintigraphic images are shown depicting tracer uptake in the heart only after myocardial infarction.

Sham: In-111-oxine labeled EPCs

Infarct: In-111-oxine labeled EPCs

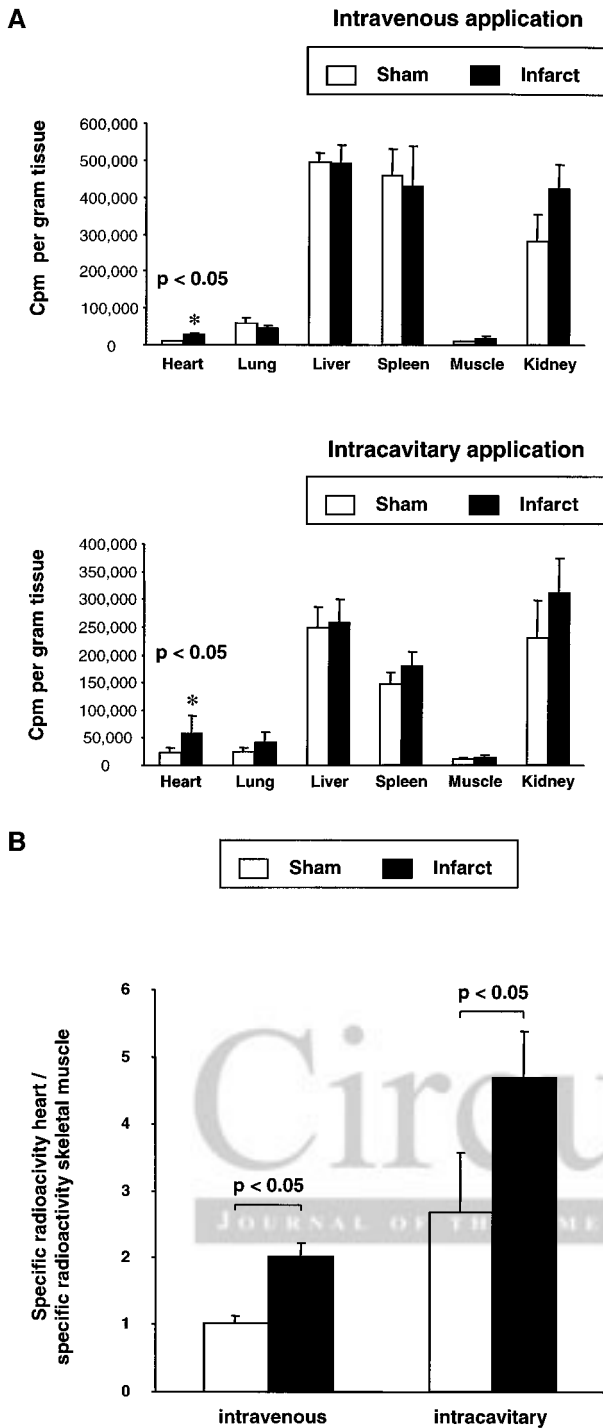


**Figure 3.** A, Distribution of radioactivity in different tissues after intravenous (top) and intracavitary (bottom) application of <sup>111</sup>In-oxine-labeled EPCs in infarct or sham-operated nude rats 96 hours after EPC therapy. B, Ratio of specific radioactivity in heart vs skeletal muscle in infarct and sham-operated animals after intravenous and intracavitary administration of <sup>111</sup>In-oxine-labeled EPCs. Data are given as mean±SD; n=8 (infarct) and n=8 (sham).

into the left ventricular cavity in rats with previous infarction (Figure 3B). The amount of radioactivity in the whole heart under these conditions corresponded to ≈3% of the injected EPCs, or ≈3×10<sup>4</sup> EPCs.

In animals treated with <sup>111</sup>In-oxine (n=3) alone, a different tracer distribution (data not shown) was observed with a high blood pool activity up to 96 hours after injection because of the strong affinity of oxine to serum transferrin. According to the scintigrams, blood samples showed a >25-fold higher specific blood activity compared with animals treated with <sup>111</sup>In-oxine-labeled EPCs.

In rats without any surgical pretreatment (n=3), no significant differences were found for the specific heart radioactivity compared with sham-operated animals. These findings exclude the operation itself as a reason for the cardiac homing of EPCs as observed in sham-operated and infarcted animals.

### Detection of EPCs by DiLDL Fluorescence and Immunostaining

To confirm the results obtained by measuring the radioactivity and to gain further insights into the morphology of the EPCs in the different tissues, tissue sections were analyzed. Therefore, EPCs were incubated with DiLDL before radioactive labeling was performed to allow for detection of DiLDL labeling in fluorescence microscopy. Moreover, EPCs were also detected by immunostaining with anti-human HLA antibodies. EPCs were rarely found in the heart of sham-operated animals (data not shown). In contrast, hearts of infarcted rats revealed positive staining for DiLDL and human HLA (48.3±21 EPCs per infarct zone; Figure 4, A and B). Consistent with previous studies,<sup>1</sup> EPCs were detected predominantly in the border zone of the infarct, as evidenced by visualizing neighboring intact cardiac myocytes with α-sarcomeric actinin (Figure 4B). The endothelial character was demonstrated further by *Ulex europaeus* lectin (Figure 4B). Of note, 96 hours after infarction, EPCs did not yet form vessel-like structures. However, when animals were killed 25 days after the EPC injection, DiLDL-labeled EPCs were integrated and revealed a differentiated phenotype (data not shown).

In addition, tissue sections of the other organs, in which the majority of the radioactivity was detected, were analyzed. In spleen, DiLDL-labeled EPCs were found predominantly in the marginal zone around lymphoid follicles and in the red pulp (Figure 4C). In contrast, in liver and kidney, DiLDL-labeled EPCs were rarely detectable, although ≈70% of the radioactivity remained in these organs. These results were confirmed by immunostaining for human HLA (data not shown).

### Discussion

The results of our study demonstrate that radiolabeling with <sup>111</sup>In-oxine is a useful method for the in vivo monitoring of the fate of infused progenitor cells. Radioactive labeling does not seem to affect cell viability or EPC function, as shown by measurements of LDH release and DiLDL uptake. Furthermore, radioactively labeled EPCs were well incorporated and revealed a differentiated phenotype in animals 25 days after infarction.

Our data reveal that the absolute level of intravenously injected EPCs homing to the heart is ≈1% of the injected radioactivity. Intravenous infusion of EPCs after infarction increased the number of EPCs in the heart significantly,

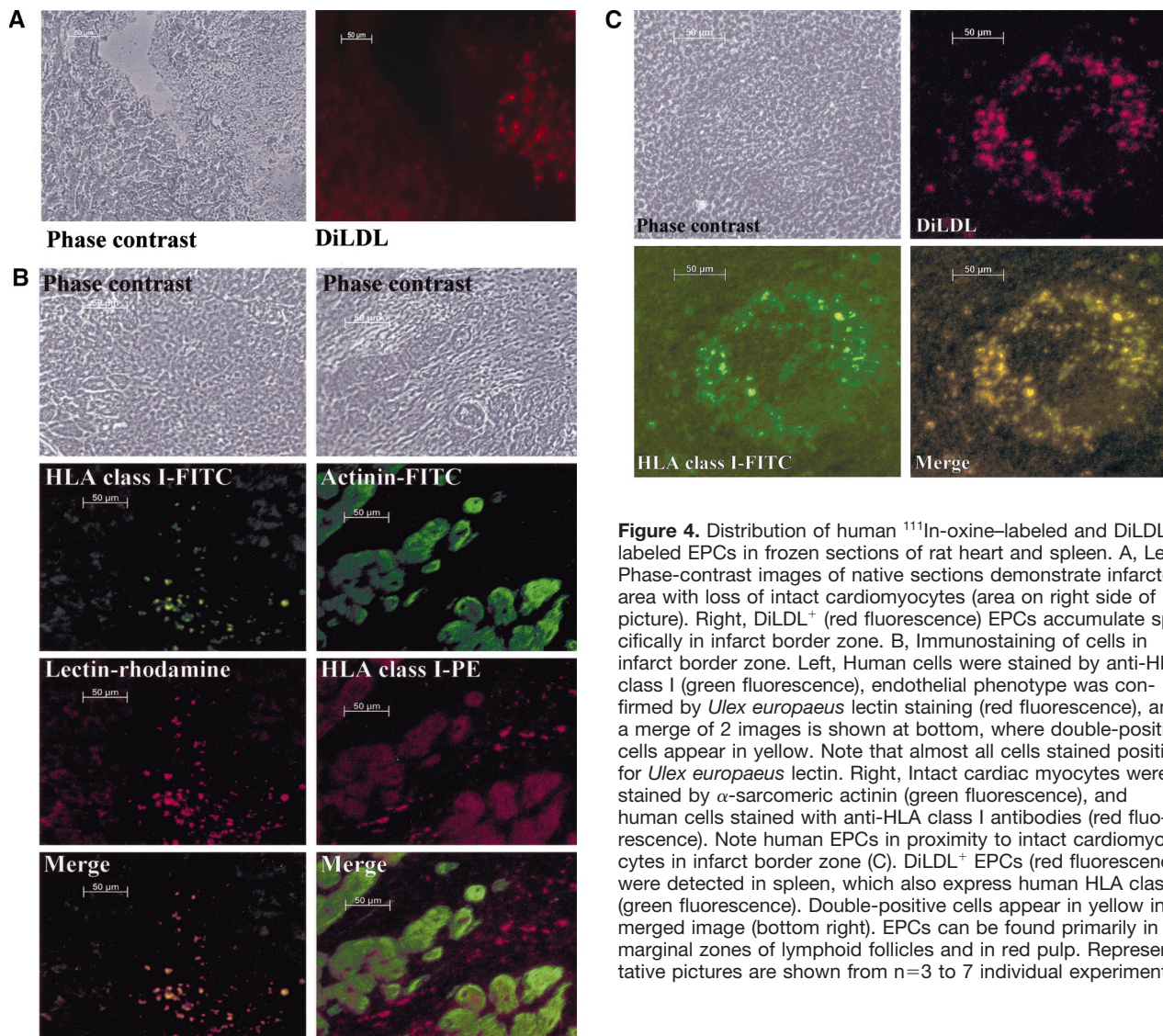


**Figure 4.** Distribution of human  $^{111}\text{In}$ -oxine-labeled and DiLDL-labeled EPCs in frozen sections of rat heart and spleen. A, Left, Phase-contrast images of native sections demonstrate infarcted area with loss of intact cardiomyocytes (area on right side of picture). Right, DiLDL<sup>+</sup> (red fluorescence) EPCs accumulate specifically in infarct border zone. B, Immunostaining of cells in infarct border zone. Left, Human cells were stained by anti-HLA class I (green fluorescence), endothelial phenotype was confirmed by *Ulex europaeus* lectin staining (red fluorescence), and a merge of 2 images is shown at bottom, where double-positive cells appear in yellow. Note that almost all cells stained positive for *Ulex europaeus* lectin. Right, Intact cardiac myocytes were stained by  $\alpha$ -sarcomeric actinin (green fluorescence), and human cells stained with anti-HLA class I antibodies (red fluorescence). Note human EPCs in proximity to intact cardiomyocytes in infarct border zone (C). DiLDL<sup>+</sup> EPCs (red fluorescence) were detected in spleen, which also express human HLA class I (green fluorescence). Double-positive cells appear in yellow in merged image (bottom right). EPCs can be found primarily in marginal zones of lymphoid follicles and in red pulp. Representative pictures are shown from n=3 to 7 individual experiments.

$\approx$ 2-fold. This is in accordance with previous studies that demonstrate that tissue ischemia is a major stimulus for incorporation of circulating progenitor cells.<sup>2–4,14,15</sup> However, even after infarction, the absolute number of EPCs detected in the heart is rather low. Thus, the number of cells that can be isolated from peripheral blood might be one major limitation for potential cell therapy. Homing of EPCs might be increased by injection of EPCs into the left ventricular cavity. Indeed, the incorporation of radioactivity into the heart in rats after myocardial infarction increased significantly, by 4.7-fold, compared with intravenous injection in sham-operated animals when EPCs were injected into the left ventricular cavity. In line with this finding, more EPCs were detectable by immunostaining and fluorescence microscopy after intracavitary injection (data not shown). One may speculate that an intracoronary infusion in humans might even further enhance the local accumulation of progenitor cells in the myocardium.

At both 1 and 96 hours after injection, radioactivity was detected predominantly in spleen, liver, and kidneys. Fluorescence microscopy and immunostaining revealed that in the

spleen, intact EPCs localized primarily to lymphoid follicles, especially around marginal zones, as expected, because the spleen is known to be the major site for homing of immunocompetent cells.<sup>16–18</sup>

In contrast, although the radioactivity was high in liver and kidneys, EPCs were rarely detectable in these organs after 96 hours. Leakage of  $^{111}\text{In}$  from labeled cells has been described to be the reason for the high uptake of radioactivity in liver and kidney.<sup>19</sup> In lymphocytes, a 70% loss of radioactivity was reported at 24 hours after cell labeling. Slightly better results were obtained in our study, with a loss of 61% of  $^{111}\text{In}$  from radiolabeled EPCs in vitro within 48 hours. Because of excretion through renal and hepatobiliary pathways, these organs exhibited a high specific activity that was not bound to EPCs, as confirmed by fluorescence microscopy and immunostaining. The nonspecific tracer signal caused by in vivo efflux of  $^{111}\text{In}$ , however, does not seem to be a major concern outside the liver and kidneys. The significant difference in specific heart uptake after myocardial infarction does indeed represent the tissue distribution of engrafted EPCs, as confirmed by colabeling of EPCs with DiLDL.

<sup>111</sup>In-oxine is a well-known, safe, and commercially available radioactive tracer for monitoring blood cells, for example, leukocytes, for inflammation scintigraphy.<sup>6</sup> Regarding the physical half-life of <sup>111</sup>In of 2.8 days, it allows us to follow up cell distribution for ≈5 to 7 days, which we considered a clear advantage over other tracers, such as <sup>99m</sup>[Tc]technetium-labeled hexamethylpropylene amine oxime (HMPAO), with a physical half-life of 6 hours. The limitation of <sup>111</sup>In, however, is its high  $\gamma$ -energy of 171 and 245 keV, which requires the use of medium-energy collimators. Although the spatial resolution (>12 mm) of these collimators is rather poor, it is sufficient for clinical application in patients. However, in nude rats with a mean weight of <200 g and a heart size just in the range of the collimator resolution, the rather low uptake of EPCs in the heart cannot be distinguished from the high tracer accumulation in the adjacent liver and spleen. An alternative to increase resolution is the use of a pinhole collimator. In our study, we could show that only pinhole collimators were appropriate tools to obtain a resolution high enough to clearly discriminate the increase in radioactivity in animals with myocardial infarctions. Moreover, for small-animal studies, the use of positron emission tomography with a high spatial resolution would be the ideal imaging modality.<sup>20</sup> However, when testing the widely available [<sup>18</sup>F]fluorodeoxyglucose as a label, an insufficient labeling efficiency of human EPCs was obtained (data not shown). <sup>64</sup>Cu has also been shown to be an alternative positron emission tomography tracer for cell labeling, with a potentially suitable half-life of 12.7 hours,<sup>21</sup> but this tracer requires generation by a cyclotron. Therefore, to extend the feasibility of progenitor cell transplantation imaging to routine clinical application, we decided to use <sup>111</sup>In-labeled EPCs, despite the limited resolution in rats, and to combine scintigraphic imaging with in vitro measurement of tissue specific activities in the heart and various other organs for this experimental setting.

In summary, the results of this study demonstrate that <sup>111</sup>In-oxine is a useful tracer for in vivo monitoring of transplanted EPCs in a rat model of myocardial infarction. Thus, radioactive labeling with <sup>111</sup>In-oxine may provide a noninvasive imaging approach to assess the fate and tissue distribution of transplanted progenitor cells during clinical cell therapy.

### Acknowledgments

This work was supported by a young investigator grant from the University of Frankfurt (Dr Aicher), a research grant from the University of Kiel (Dr Brenner), and by research grants (Di 600/4-1) from the Deutsche Forschungsgemeinschaft (Dr Dimmeler). We thank Christiane Mildner-Rihm, Marion Muhly-Reinholz, and Kerstin Brötzmann for excellent technical assistance. We are grateful for the use of the animal surgery facilities at the Department of General and Thoracic Surgery and are indebted to Rosemarie Grams (Department of Obstetrics and Gynecology), Dr Hans-Ulrich Wottge

(Animal Center), and Kerstin Gelhaus (Department of Pathology), all at the University of Kiel.

### References

1. Kawamoto A, Gwon HC, Iwaguro H, et al. Therapeutic potential of ex vivo expanded endothelial progenitor cells for myocardial ischemia. *Circulation*. 2001;103:634–637.
2. Kalka C, Masuda H, Takahashi T, et al. Transplantation of ex vivo expanded endothelial progenitor cells for therapeutic neovascularization. *Proc Natl Acad Sci U S A*. 2000;97:3422–3427.
3. Iwaguro H, Yamaguchi J, Kalka C, et al. Endothelial progenitor cell vascular endothelial growth factor gene transfer for vascular regeneration. *Circulation*. 2002;105:732–738.
4. Shintani S, Murohara T, Ikeda H, et al. Augmentation of postnatal neovascularization with autologous bone marrow transplantation. *Circulation*. 2001;103:897–903.
5. Zhang ZG, Zhang L, Jiang Q, et al. Bone marrow-derived endothelial progenitor cells participate in cerebral neovascularization after focal cerebral ischemia in the adult mouse. *Circ Res*. 2002;90:284–288.
6. Becker W, Meller J. The role of nuclear medicine in infection and inflammation. *Lancet Infect Dis*. 2001;1:326–333.
7. Seabold JE, Forstrom LA, Schauwecker DS, et al. Procedure guideline for indium-111-leukocyte scintigraphy for suspected infection/inflammation. *J Nucl Med*. 1997;38:997–1001.
8. Rennen HJ, Boerman OC, Oyen WJ, et al. Imaging infection/inflammation in the new millennium. *Eur J Nucl Med*. 2001;28:241–252.
9. Bohnen NI, Charron M, Reyes J, et al. Use of indium-111-labeled hepatocytes to determine the biodistribution of transplanted hepatocytes through portal vein infusion. *Clin Nucl Med*. 2000;25:447–450.
10. Mackensen A, Krause T, Blum U, et al. Homing of intravenously and intralymphatically injected human dendritic cells generated in vitro from CD34+ hematopoietic progenitor cells. *Cancer Immunol Immunother*. 1999;48:118–122.
11. Eggert AA, Schreurs MW, Boerman OC, et al. Biodistribution and vaccine efficiency of murine dendritic cells are dependent on the route of administration. *Cancer Res*. 1999;59:3340–3345.
12. Vasa M, Fichtlscherer S, Adler K, et al. Increase in circulating endothelial progenitor cells by statin therapy in patients with stable coronary artery disease. *Circulation*. 2001;103:2885–2890.
13. Vasa M, Fichtlscherer S, Aicher A, et al. Number and migratory activity of circulating endothelial progenitor cells inversely correlate with risk factors for coronary artery disease. *Circ Res*. 2001;89:E1–E7.
14. Takahashi T, Kalka C, Masuda H, et al. Ischemia- and cytokine-induced mobilization of bone marrow-derived endothelial progenitor cells for neovascularization. *Nat Med*. 1999;5:434–438.
15. Shintani S, Murohara T, Ikeda H, et al. Mobilization of endothelial progenitor cells in patients with acute myocardial infarction. *Circulation*. 2001;103:2776–2779.
16. Iezzi G, Scheidegger D, Lanzavecchia A. Migration and function of antigen-primed nonpolarized T lymphocytes in vivo. *J Exp Med*. 2001;193:987–993.
17. Patel SS, Thiagarajan R, Willerson JT, et al. Inhibition of  $\alpha_4\beta_1$  integrin and ICAM-1 markedly attenuate macrophage homing to atherosclerotic plaques in ApoE-deficient mice. *Circulation*. 1998;97:75–81.
18. Hendrikx PJ, Martens CM, Hagenbeek A, et al. Homing of fluorescently labeled murine hematopoietic stem cells. *Exp Hematol*. 1996;24:129–140.
19. Kuyama J, McCormack A, George AJ, et al. Indium-111 labelled lymphocytes: isotope distribution and cell division. *Eur J Nucl Med*. 1997;24:488–496.
20. Wu JC, Inubushi M, Sundaresan G, et al. Positron emission tomography imaging of cardiac reporter gene expression in living rats. *Circulation*. 2002;106:180–183.
21. Adonai N, Nguyen KN, Walsh J, et al. Ex vivo cell labeling with <sup>64</sup>Cu-pyruvaldehyde-bis(N4-methylthiosemicarbazone) for imaging cell trafficking in mice with positron-emission tomography. *Proc Natl Acad Sci U S A*. 2002;99:3030–3035.